

The depositional setting of the Late Quaternary sedimentary fill in southern Bannu basin, Northwest Himalayan fold and thrust belt, Pakistan

Asam Farid · Perveiz Khalid · Khan Zaib Jadoon ·
Mohammed Soufiane Jouini

Received: 8 December 2013 / Accepted: 11 June 2014 / Published online: 10 July 2014
© Springer International Publishing Switzerland 2014

Abstract Geostatistical variogram and inversion techniques combined with modern visualization tools have made it possible to re-model one-dimensional electrical resistivity data into two-dimensional (2D) models of the near subsurface. The resultant models are capable of extending the original interpretation of the data to depict alluvium layers as individual lithological units within the 2D space. By tuning the variogram parameters used in this approach, it is then possible to visualize individual lithofacies and geomorphological features for these lithologic units. The study re-examines an electrical resistivity dataset collected as part of a groundwater study in an area of the Bannu basin in Pakistan. Additional lithological logs

from boreholes throughout the area have been combined with the existing resistivity data for calibration. Tectonic activity during the Himalayan orogeny uplifted and generated significant faulting in the rocks resulting in the formation of a depression which subsequently has been filled with clay-silt and dirty sand facies typical of lacustrine and flood plain environments. Streams arising from adjacent mountains have reworked these facies which have been eroded and replaced by gravel-sand facies along channels. It is concluded that the sediments have been deposited as prograding fan shaped bodies, flood plain, and lacustrine deposits. Clay-silt facies mark the locations of paleo depressions or lake environments, which have changed position over time due to local tectonic activity and sedimentation. The Lakki plain alluvial system has thus formed as a result of local tectonic activity with fluvial erosion and deposition characterized by coarse sediments with high electrical resistivities near the mountain ranges and fine sediments with medium to low electrical resistivities towards the basin center.

A. Farid · P. Khalid
Institute of Geology, University of Punjab,
P.O. Box 54590, Lahore, Pakistan

P. Khalid
e-mail: perveiz.geo@pu.edu.pk

A. Farid (✉)
Department of Petroleum Geosciences, The Petroleum
Institute,
P.O. Box 2533, Abu Dhabi, United Arab Emirates
e-mail: asam.farid@gmail.com

K. Z. Jadoon
Water Desalination and Reuse Center, King Abdullah
University of Science and Technology (KAUST),
Thuwal 23955-6900, Saudi Arabia
e-mail: khan.jadoon@kaust.edu.sa

M. S. Jouini
Department of Mathematics, The Petroleum Institute,
P.O. Box 2533, Abu Dhabi, United Arab Emirates
e-mail: mjouini@pi.ac.ae

Keywords Bannu · Gambila · Variogram · Facies ·
Paleogeomorphology

Introduction

Many significant valley systems within the Northwest Himalayan region are products of regional and local tectonic activity rather than of fluvial or glacial processes. During the various episodes of orogeny since the Late Cretaceous when the Indian and Eurasian plates

initially collided, the uplift of mountain masses has resulted in the formation of a number of intermontane basins. The sediments created by the erosion of these mountains are carried into these basins under the action of sedimentary processes forming talus slopes, alluvial fans, alluvial deposits, and lacustrine deposits. The grain size of the sediments may range from very coarse alluvial fan gravels and channel deposits, with high hydraulic conductivities to very fine lacustrine clays, with low hydraulic conductivity. Therefore, the lithologic and geomorphic nature of the sediments plays an important role in the development of clastic fluvial aquifers and their hydraulic characteristics such as transmissivity, hydraulic conductivity, and specific yield (Bowling et al. 2005).

Thus, the ability to identify and characterize the lithologic and geomorphic relationships of the sedimentary deposits is an essential element for efficient groundwater resource management. However, characterization of lithology is difficult to achieve in many alluvial systems when systems have variable lithologic and geomorphic composition, especially with irregular grain sizes and sorting occurrence. The study of such fluvial systems can prove challenging due to the highly variable lithologies, which may grade between clay to gravel, poorly sorted to nearly homogenous facies, and facies with thicknesses ranging from just a few centimeters to whole channel fills. Where available, borehole data can provide useful additional information to resolve such issues; however, in places where the lithologies become highly variable then, direct observational methods such as drilling boreholes become impractical in terms of time and cost as well as environmental impact. Alternatively, surface geophysical methods can provide a more efficient approach in surveying over large spatial areas. Previous studies on the topic have reported a multitude of geophysical methods being employed to characterize a wide variety of aquifer types with varying degrees of success. The primary objective of these studies has been to quantify the physical properties that are closely related to the observed variations in hydraulic conductivity, such as lithology, fracture distribution, porosity, and permeability (Bowling et al. 2007). Typical geophysical methods employed in such surveys have included geoelectric, geomagnetic, seismic, gravity, geothermometry, well logging, and natural radiation detection (Vogelsang 1995).

Electrical resistivity has long been used as a method to detect the subsurface hydrogeological and

geomorphological features with considerable success (Stewart et al. 1983; Courteaud et al. 1997; Louis et al. 2002; Zouhri et al. 2004; Schrott and Sass. 2008; Edmund 2009; Okoro et al. 2010; Riddell et al. 2010; Akhter et al. 2012). Electrical resistivity in addition to the lithologic makeup of the aquifer depends upon the fluid contents of the aquifer. In fresh groundwater conditions, the electrical resistivity method can provide an effective indicator of the clay content of the aquifer system. However, as groundwater conditions become increasingly saline then the resistivity method is less reliable for the detection of lithologies. Thus, when deploying geoelectrical methods on groundwater systems, the salinity of the groundwater will limit the accuracy in determining the lithology of the aquifer. In general, clays will appear as good electrical conductors with coarser sediments tending to be more resistive.

A variogram is an important geostatistical tool for measuring the variability of spatially sampled data and is used in the gridding and modeling process. The derived “variability” value increases as the input samples become more disparate. The more basic and popular gridding algorithms such as “least squares” and “minimum curvature” tend to be insensitive to trends in the data, and apart from the ability to manually set the parameters such as the node separation distance and search radii, they lack the ability to be “tuned” to fit the dataset. Alternatively, variogram gridding and interpolation techniques are capable of far greater compliance with the observed data, but this method requires that an analytical model be input in order to produce surfaces capable of reflecting the geometry and continuity of the studied phenomenon. Thus, the resultant output incorporates an intuitive level of understanding of the spatial trends inherent in the data, forming an important aid during the interpretation process (Journel and Huijbregts 1978; Armstrong 1984; Cressie 1993; Olea 1995; Goovaerts 1997; Gringarten and Deutsch 2001). The geostatistical variogram has therefore become an essential technique for correlating and quantifying the spatial relationships found in discretely sampled data and has thus been employed in this study to improve the quality of the interpretation.

Regional subduction of the Indian continental plate below the Eurasian plate has caused uplift and significant bedrock faulting as the Himalayan orogeny has progressed. The deformation of rocks in the region has resulted in the formation of depressions, which have been filled with sediments derived from the erosion of

the adjacent mountains (Kazmi and Jan 1997; Shahzad et al. 2009, 2010). The processes of weathering, erosion, and deposition have resulted in the deposition of complex alluvial facies in the study area. This study attempts to delineate and map the alluvial facies sequences by applying geostatistical techniques to vertical electrical soundings (VES) data in an intermontane basin environment.

General geology and geomorphology

Bannu basin is located as a depression behind the present-day trans-Indus uplift boundary, which results in the formation of Bhattani, Khisor/Marwat, and Shinghar ranges. Bannu basin was formed by the southward migration of the uplift boundary from the Kohat ranges to the Bhattani and Marwat/Khisor ranges and is encircled by mountains on all sides as shown in Fig. 1. To the north, the basin is bounded by the Kohat ranges; to the northeast, the Shingar range; to the southeast, the Marwat range; to the southwest, the Bhattani range; and to the west, by the Waziristan-Sulaiman range. The Bannu area was part of the large Indo-Gangetic foreland basin until its disruption by the uplift of the Bhattani and Marwat/Khisor ranges, about 500,000 years ago. The highest peaks of the ranges near to the study area reach heights of 1,943 m in the Bhattani range and 1,376 m at the southwestern tip of the Marwat range (Dalfsen et al 1986). In the study area, the ground surface elevation decreases from a level of around 600 m in the extreme western part to about 225 m toward the east with the Kurram River being the main stream passing through the basin. The second major stream of the area is Gambila River, which enters the basin southwest of Bannu, and then runs southeast for most of its course and after curving eastward falls into the Kurram east of Lakki (Dalfsen et al 1986). Apart from the above perennial streams, there are several ephemeral streams which only after rainstorms carry surface runoff toward the Gambila and Kurram Rivers.

The study area occupies the southern part of the Bannu basin. Its northern boundary is defined by the course of the Gambila River as shown in Fig. 2. Elsewhere, it is surrounded by the Marwat, Bhattani, and Waziristan-Sulaiman ranges. The study area lies between latitudes 32.35° N to 33° N and longitudes 70.33° E to 71.16° E. Landforms of the area show erosion by incision of streams, as is evident from their

deeply eroded channels as shown in Fig. 3. The investigated area is known for its very hot summers and mild winters, weather being predominantly dry and sunny, with the occasional gales and dust storms. The sedimentary rocks exposed in the Bhattani and Marwat ranges as shown in Fig. 4 underlie a considerable part of the investigated area.

Subsurface lithologies as shown in Fig. 5 are highly variable ranging from very coarse-grained sediments such as gravels and boulders, to very fine sediments such as silt and clays. There are three broad types of sediment evident in the study area including alluvial fan, flood plain, and basin fill sediments. The alluvial fan sediments constitute the mixtures of boulders, gravels, sand, silt, and clay in various proportions. The flood plain deposits are mainly clay and silt with some sand. The sandy deposits mainly form along the Marwat range and are predominantly the result of the erosion of these ranges.

Methods

Electrical resistivity survey

Between April 1983 and April 1984, the Water and Power Development Authority (WAPDA) under Pak-Dutch program acquired the VES dataset as part of an investigation to gather accurate information about the hydrogeology of the area. To cover the entire area, a total of 382 VES were performed, adopting the Schlumberger configuration with half electrode spacing (AB/2) ranging from 3 to 1,600 m. For convenience, the VES were generally collected at a distance (sampling interval) of approximately 1 km, mostly along existing roads and tracks (Dalfsen et al 1986).

Interpretation of VES curves requires that the measured curve be matched against several model curves, each of which represents different subsurface resistivity distributions. Therefore, the selection of the final interpretive model is constrained by the available hydrogeological information. The most useful information includes subsurface lithology, groundwater levels, and distribution of electrical conductivities (EC). The water table elevation map for the area is shown in Fig. 6. The original VES data has been modeled using the IPI2WIN software (IPIWIN-1D 2000; Zananiri et al. 2006; Sultan et al. 2009; Farid et al. 2013) utilizing information derived from lithologic logs, geologic

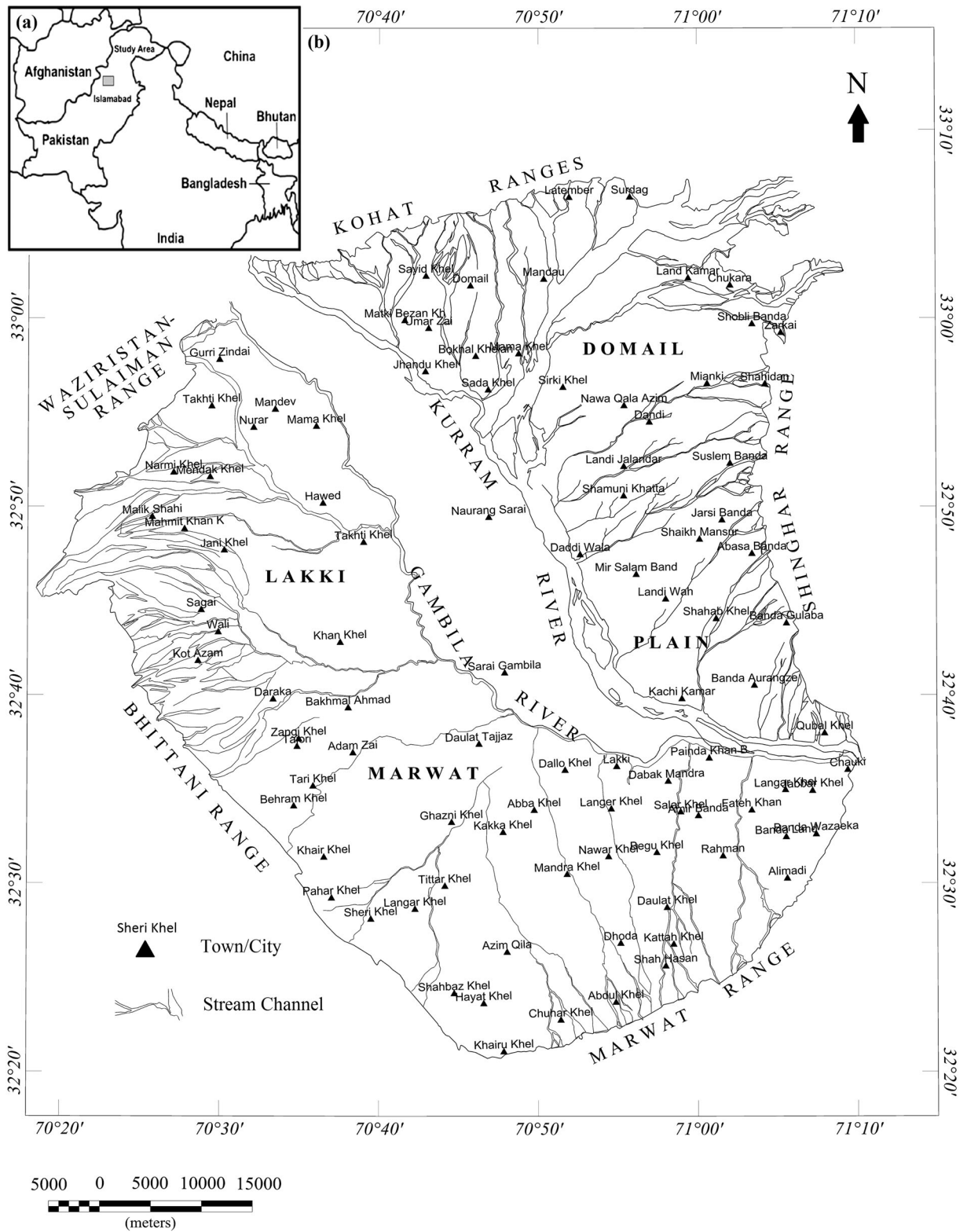


Fig. 1 a The regional location of Bannu Basin. b Physiography of the Bannu Basin

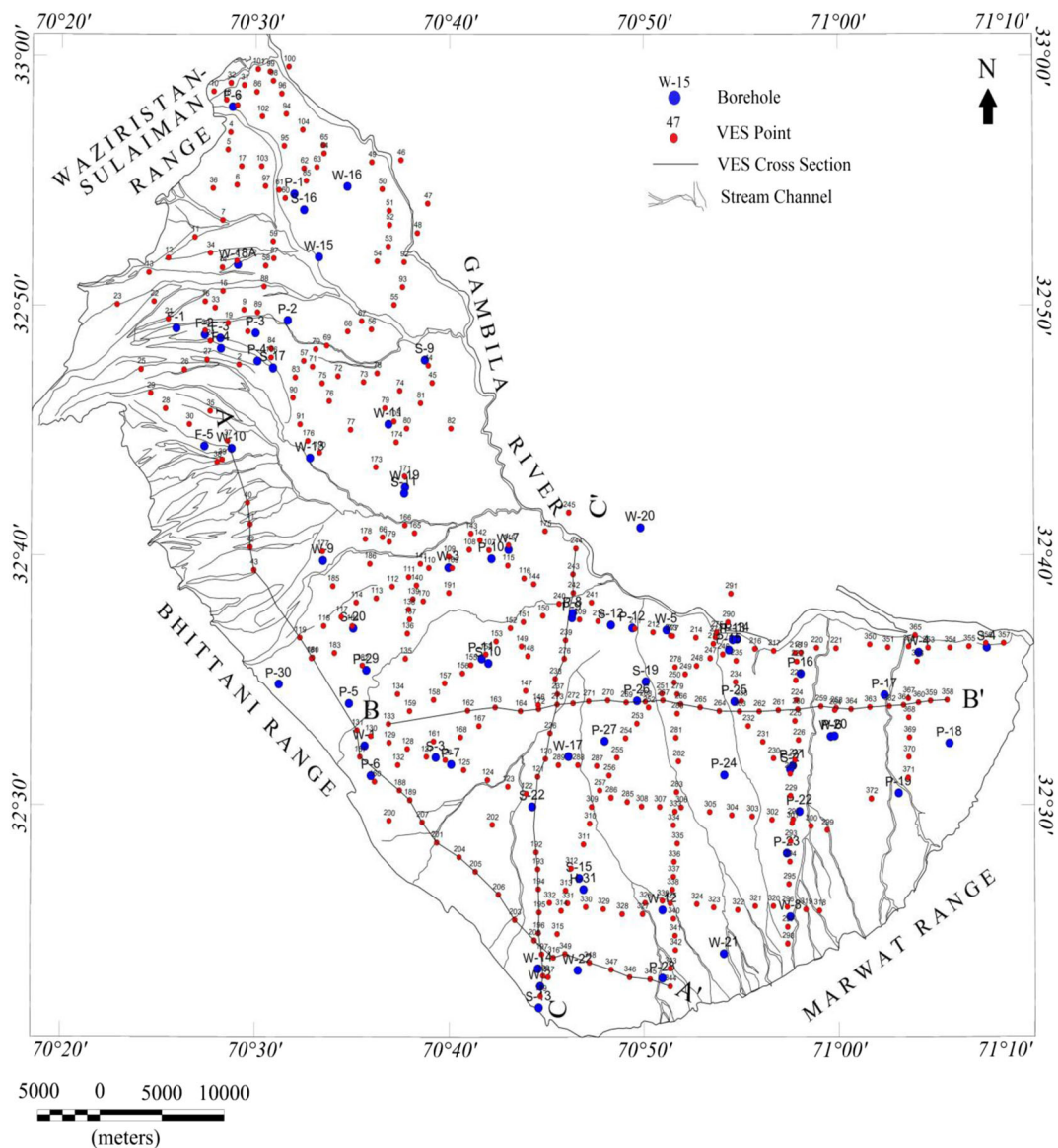


Fig. 2 Location of exploratory boreholes, VES points, study area boundaries, and cross-section profiles (after Dalfsen et al 1986)

maps, data on subsurface water levels, and EC. The measured apparent VES curve and interpreted (modeled) curves are shown in Fig. 7. The small circles in Fig. 7 represent the sampled resistivity at a particular depth with the black line representing the line of best fit for the apparent resistivity and the blue line representing the modeled true resistivity. The x-axis represents both the current electrode spacing (AB/2) for the apparent resistivity and depth (m) for the modeled resistivity curve, respectively. The resistivity values plotted against depth are schematized into a resistivity model consisting

of sequences of horizontal layers differentiated according to discrete bands resistivity as shown in Fig. 7a–d. General calibration between lithology and resistivity is established using the borehole information and resistivity data and is shown in Table 1, with the information detailed in Table 1 has been used to interpret all of the VES curves and developing layer models. Each model’s response curve represents the simulated VES response of a horizontally stratified earth using a limited number of sedimentary layers (three to eight) with the base layer extending to infinite depth. Each of these layers is

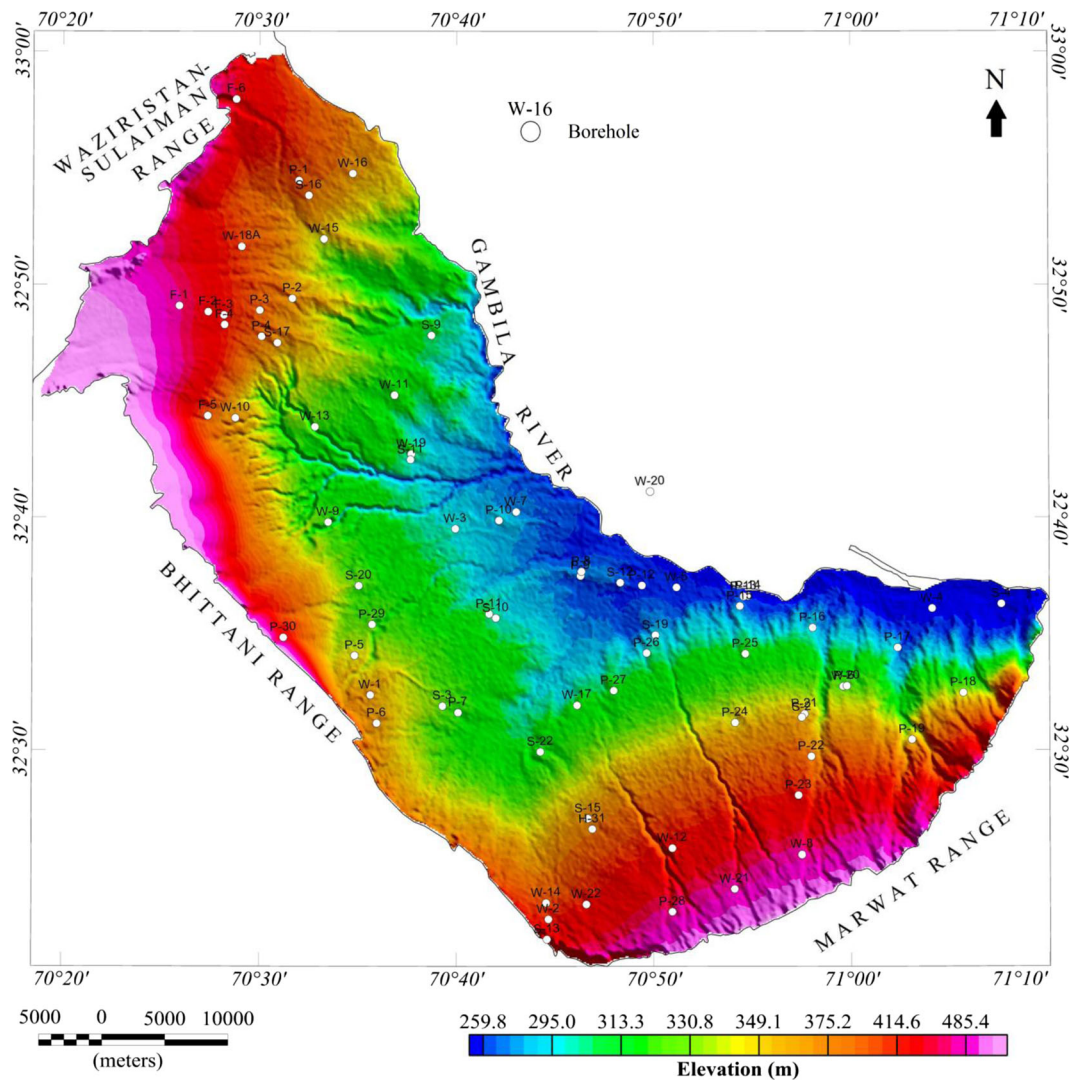


Fig. 3 Digital elevation model of the study area (data source: Geosoft 2013)

characterized by its electrical resistivity and thickness except for the base layer, which has an indefinite thickness. The interpreted resistivity layer models together provide a model of the subsurface electrical resistivity field to be pictured schematically in depth.

Resistivity of groundwater varies in the study area as shown in Fig. 8. The resistivity of groundwater ranges between less than $5 \Omega\text{m}$ and greater than $20 \Omega\text{m}$. For this study, groundwater with resistivity of $5 \Omega\text{m}$ or less is considered saline. Saline groundwater is mostly found at shallow depths mostly in artesian conditions except between wells W-14 and W-22, where it extends in greater depths.

Variograms

A variogram is an important geostatistical tool for measuring the variability of spatially sampled data and is used in the gridding and modeling process. The derived “variability” value increases as the input samples become more disparate. Most basic and popular gridding algorithms such as “least squares” and “minimum curvature” are insensitive to trends in the data, and apart from the node distance and search radii parameters, lack the ability to be “tuned” to fit the data.

Variogram gridding and interpolation techniques require an analytical model as input in order to produce surfaces capable of reflecting the geometry and

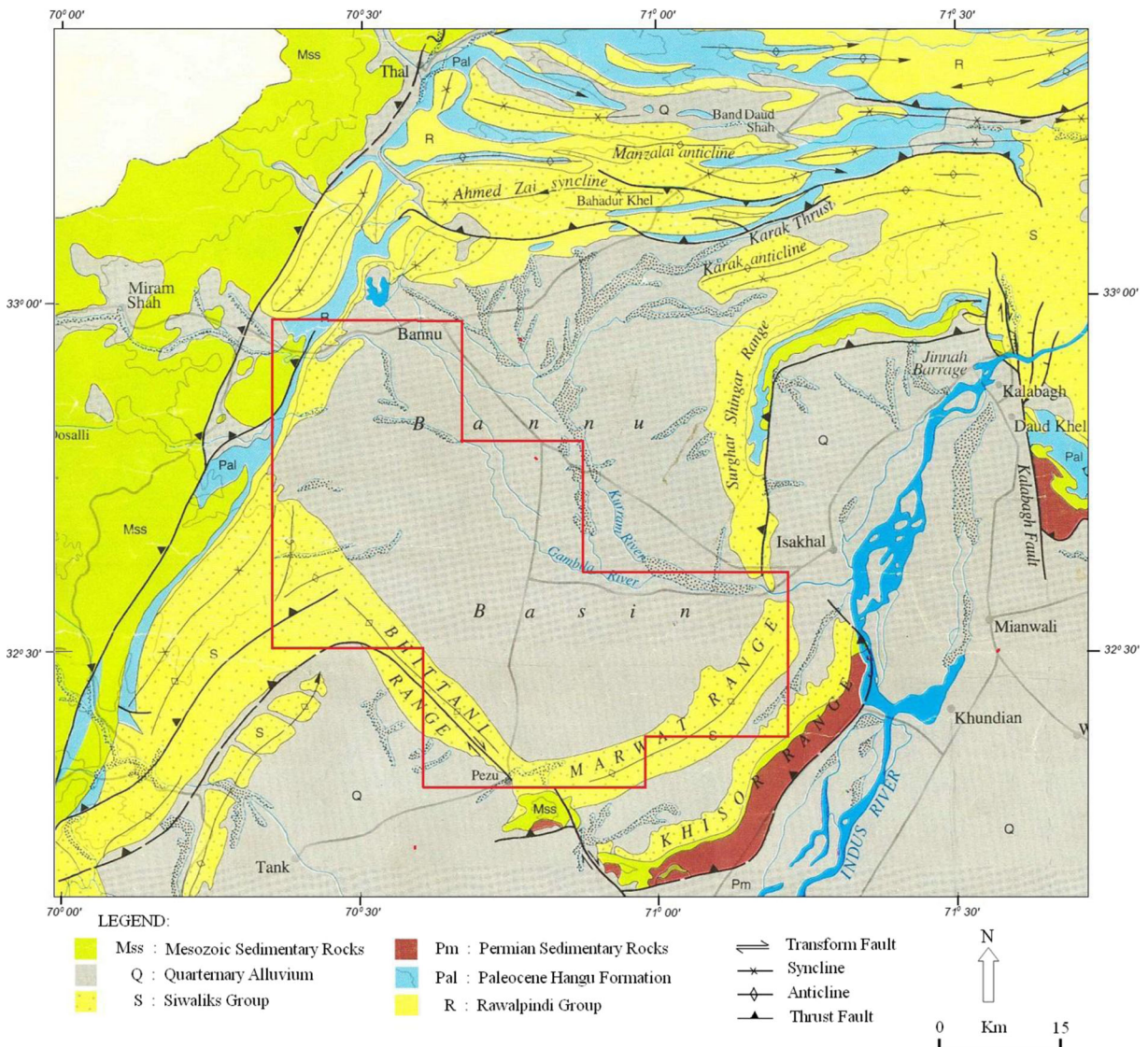


Fig. 4 Regional geology of study area (Searle et al. 1996). Study area highlighted in red color

continuity of the studied phenomenon. Hence the resultant output incorporates a level of understanding of the spatial trends inherent in the data, which forms an important aid during the interpretation process. Thus, the geostatistical variogram has become an essential technique for correlating and quantifying the spatial relationships found in discretely sampled data.

The variogram (or in this simplified case the “semivariogram”) is calculated using the following expression,

$$X(h) = 0.5 \times E[Z(X+h) - Z(x)]^2$$

Where $X(h)$ is the semivariance or variability, E is the expectation, X is the location, h is the sampling distance, and Z is the observed data value. The above expression provides a measure of correlation between the sampled values and their range of scatter.

As the distance between samples approaches zero (i.e., $h \rightarrow 0$), the value of the variogram should also approach zero. However, should the variogram be greater than zero in this situation then any residual value is defined as the “nugget effect” (C_0) as shown in Fig. 9. The total sill (S) of the variogram is then calculated as, $C + C_0$. Often C is also treated equal to the S of the

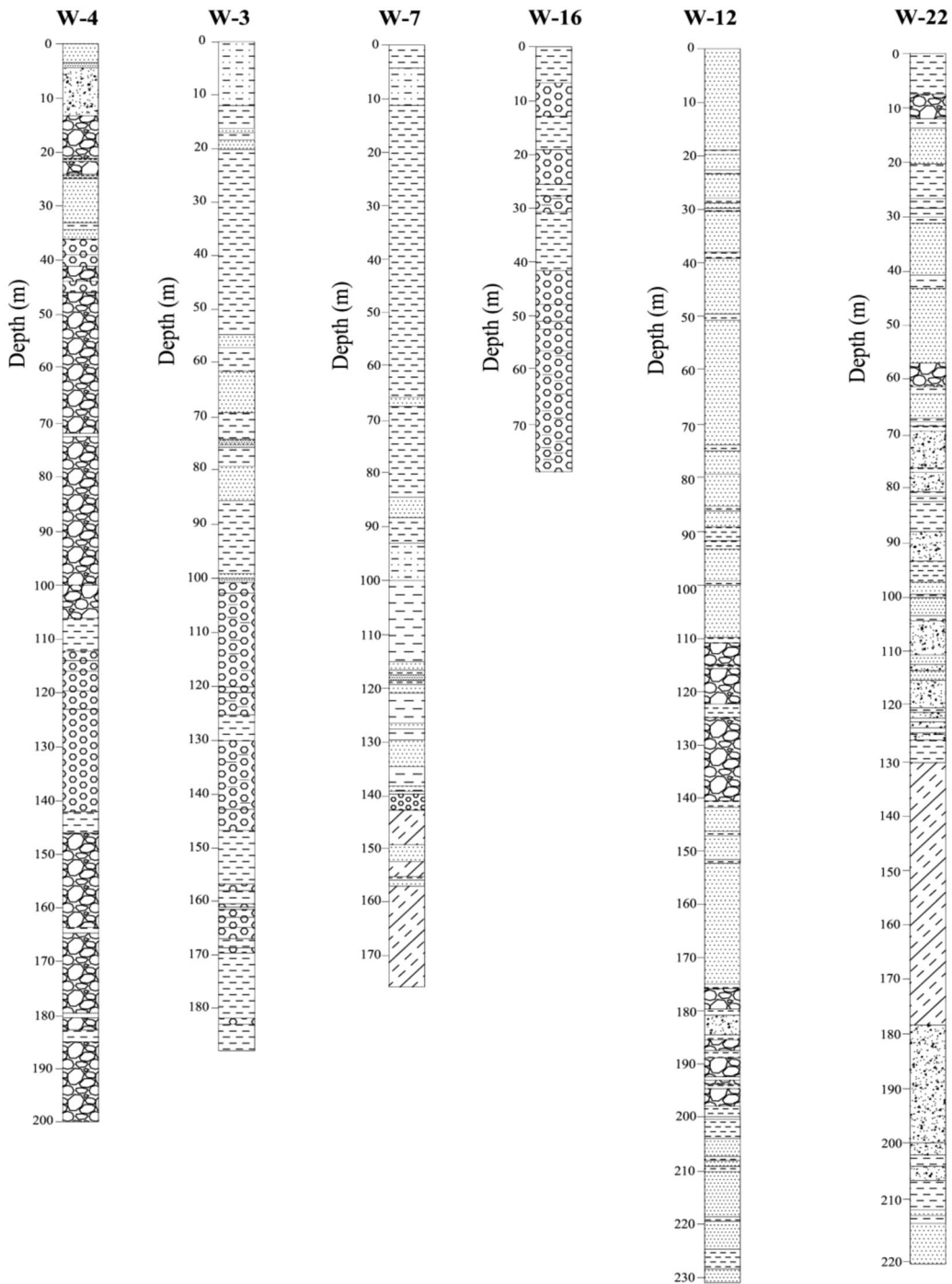


Fig. 5 Lithologs of boreholes W-4, W-3, W-7, W-16, W-12, and W-22. Lithologs describe the variable subsurface lithologies

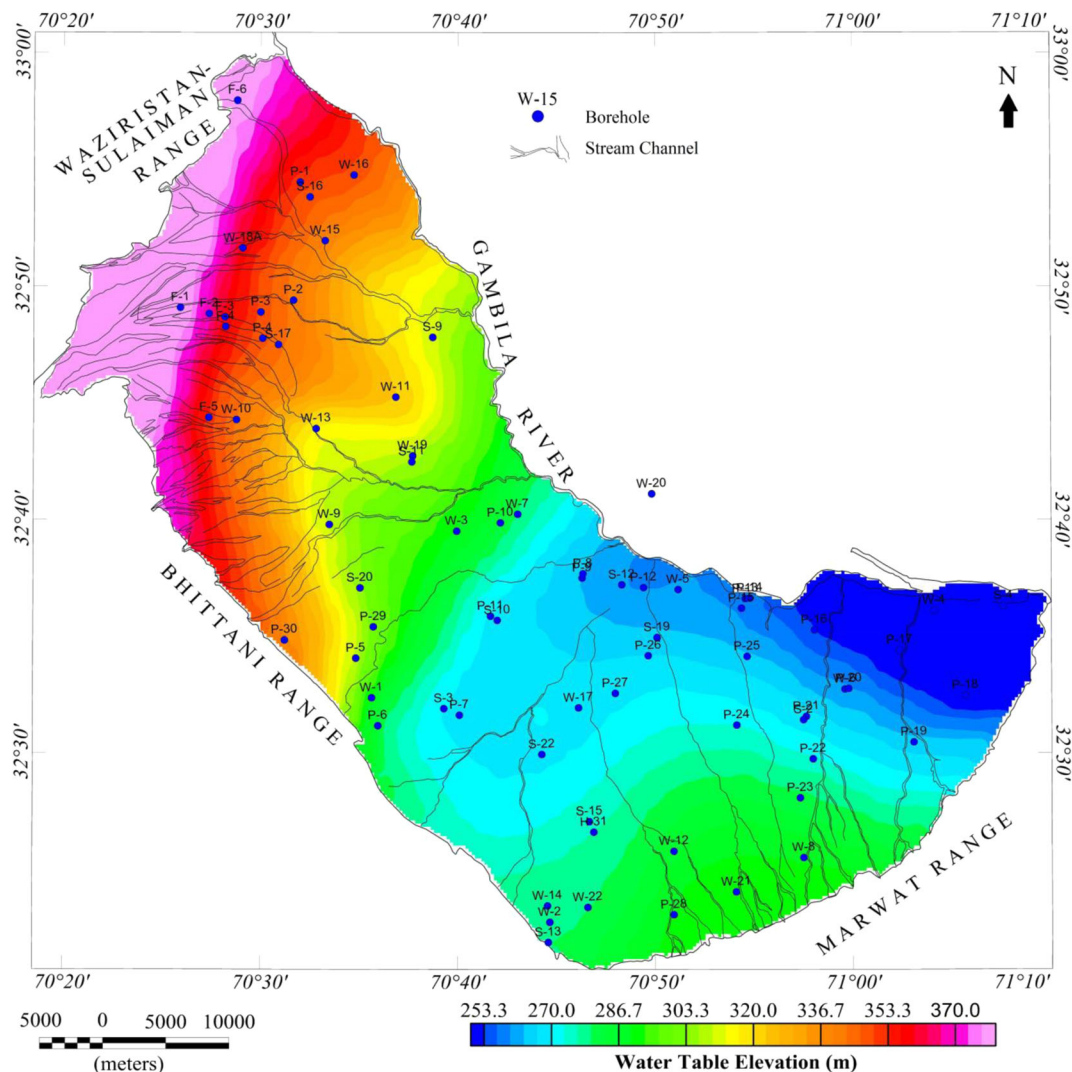


Fig. 6 Water table elevations (after Dalfsen et al 1986)

variogram model fitted to the experimental variograms when C_0 is zero.

There are many possible variogram model types, which can be applied in the calculation; these include linear, gaussian, exponential, and spherical models. For most datasets, any of these basic models types will deliver an adequate result, and for this study, the spherical model was selected.

The spherical model is given as:

$$X(h) = C_0 + (C - C_0) \left[(1.5h) / \left(\alpha + 0.5 \left(h / \alpha \right)^3 \right) \right]$$

Where α is the range of the variogram.

Kriging requires the use of a model of the variogram in order to determine the weighting factors to be used in the kriging matrix as the statistical accuracy is related to how closely the model reflects the observed variogram. Kriging is the gridding technique which takes into consideration the trends in the data, i.e., the spatial variations in the datasets. It is important to smooth the line of best fit through $X(h)$ and also to ensure that it is increasing with h until it reaches the S of the variogram.

As this dataset is relatively sparse (approximately 1 km sampling interval), considerable interpolation is required to build the resistivity field over the entire study area. In order to intelligently predict values between sample points, most gridding techniques will take some

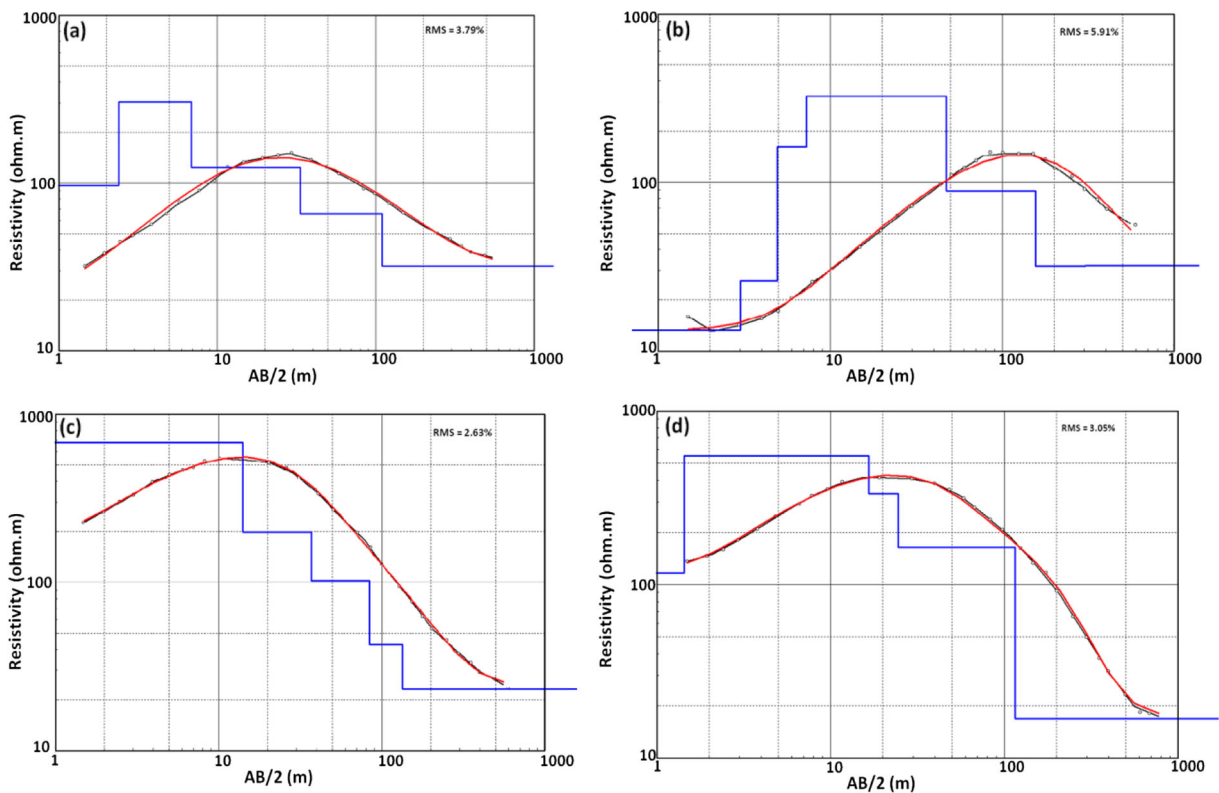


Fig. 7 a–d Apparent resistivity data are marked by *small circles*. *Solid black curve* represents the apparent resistivity curve. *Red curve* is the best-fitted curve to the apparent resistivity data. *Solid*

blue block line is the modeled resistivity (synthetic resistivity). *Horizontal axis* is the current electrode spacing (AB/2) in meters, and *vertical axis* is the resistivity in ohm meters

form of weighted averaging approach to interpolating values at grid nodes, in this case linear weighted average is used, i.e.,

$$T = w_1g_1 + w_2g_2 + w_3g_3 + \dots + w_mg_m$$

Where $g_1, g_2, g_3, \dots, g_m$ is the sampled resistivity, $w_1, w_2, w_3, \dots, w_m$ are the weighting factors for the resistivity, and T is the property to be assigned.

Table 1 Calibration between different lithologies and resistivity

Lithology	Resistivity (Ωm)	Water table
Gravel-sand	>200	Above water table
Gravel-sand	25–200	Below water table
Clay-silt	<15	Below water table
Clay-silt	<15	Above water table
Dirty sand	15–25	Below water table
Saline sediment	<5	Below water table

Results and discussion

This work interrelate the geophysical and geostatistical methods of data analysis. The VES was acquired and processed using industry standard procedures but has been visualized using modern geostatistical techniques and software. The visualizations of the geostatistically enhanced data make it possible to interpret the depositional setting of the study area.

Variations in resistivity and lithology

The lithology and resistivity calibration has been schematized into two separate zones as shown in Table 1; a near-surface zone above the water table and a deeper zone below the water table. The highest resistivity ranges (Res > 200 Ωm) that occur above water table are associated with the dry gravel-sand sediments termed as gravel-sand facies. These are observed along the mountain ranges, which reflect the sediments eroded from the mountains having been transported for great

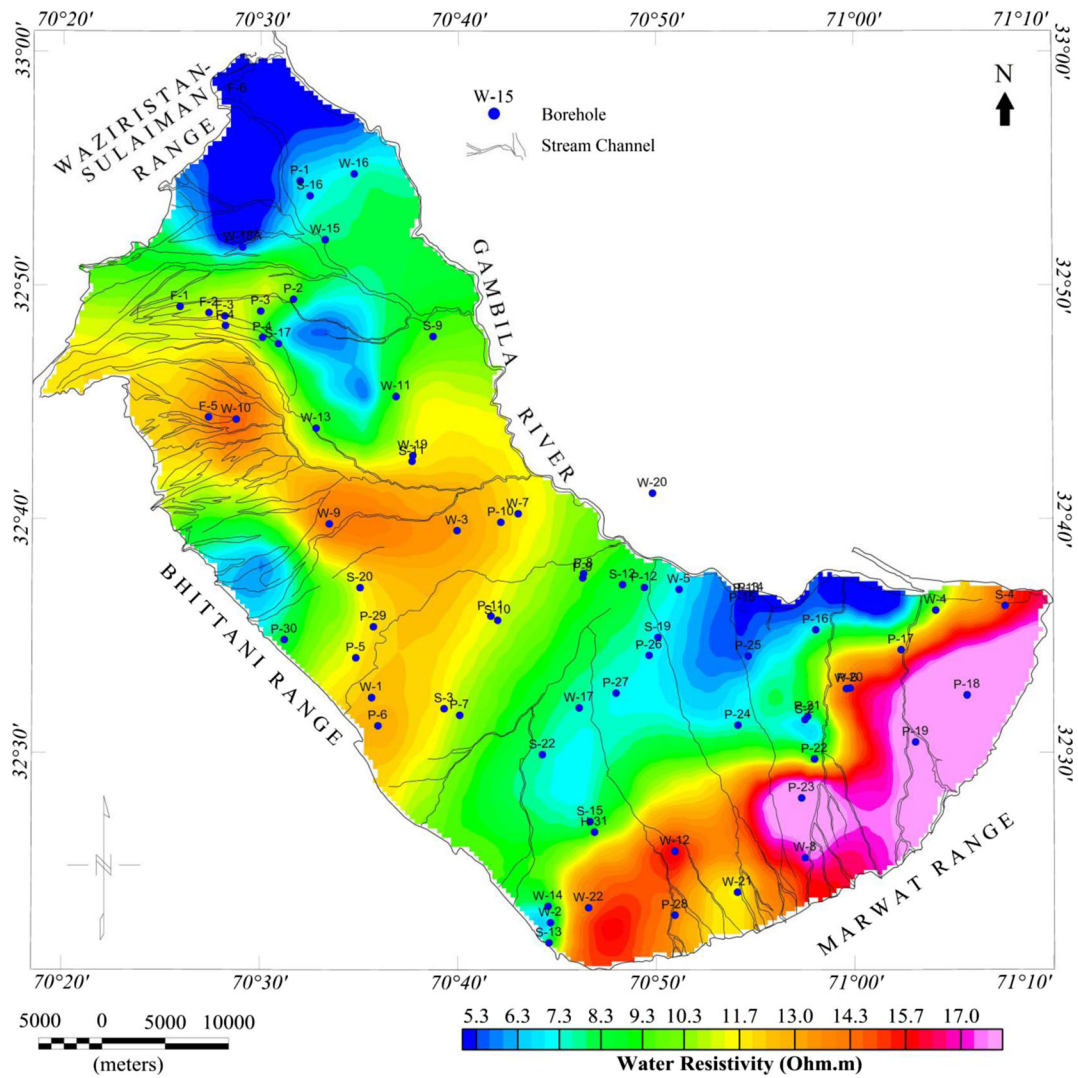


Fig. 8 Distribution of water resistivity in the study area

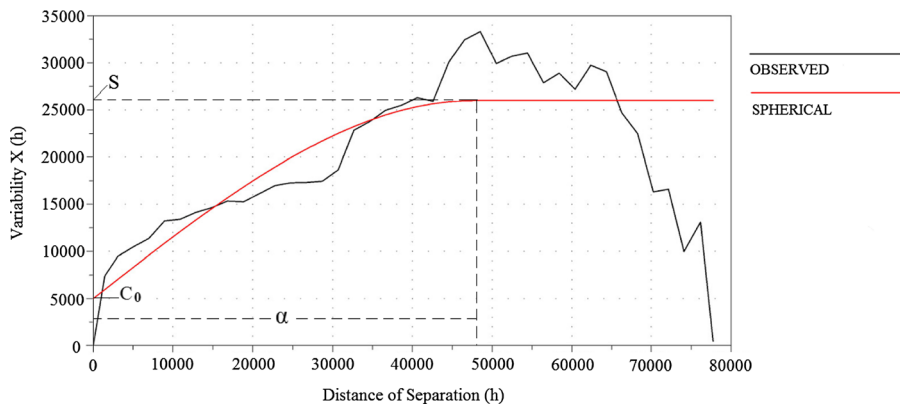


Fig. 9 Variogram

distances and hence have variable grain sizes and poor sorting. The resistivity range ($15 > \text{Res} < 25 \Omega\text{m}$) measured from below water table are associated with mixtures of silt, clay, and sand, which are widely distributed throughout the basin and are termed “dirty sand facies” in this paper. The lowest resistivity ranges ($\text{Res} < 15 \Omega\text{m}$) above and below water table are associated with interlayered clay and silt sediments termed as “clay-silt facies.” These facies are more concentrated towards the centre of the basin. The intermediate resistivity ranges ($25 > \text{Res} < 200 \Omega\text{m}$) are assigned to water-saturated gravel and sand sediments, which constitutes the major aquifer in the area.

Depositional setting

The variogram parameters as presented in Table 2 assigned for the subsurface resistivities at various depths. The nugget % (spatial ratio) shows the “spatial class” factor, which is assigned to distinguish between classes of spatial dependence in the study area. A ratio which is $<25\%$, has variable (resistivity) considered strongly spatially dependent; if the ratio is between 25 and 75 %, the resistivity is considered to be moderately spatially dependent and if the ratio is $>75\%$ then the resistivities are considered weakly spatially dependent (Cambardella et al. 1994; Iqbal et al. 2005). The resultant variograms shown in the corresponding figures indicate the existence of a strong spatial dependence for the resistivity at all the observed depths with the highest value of 26.72 % being close to 25 % as shown in Table 2. A general spatial structure is seen in Fig. 10 where the difference between sill and nugget is minimal almost flattening out around 100 m depth. This is attributed to a change in depositional event, which resulted in changing the depositional environment from flood plain to lacustrine. The structural dependence is stronger with depth, due to general widening of the dirty sand facies and their corresponding resistivities. This results in a

lower sill value but higher range values in the corresponding variograms. Krigging was used as the algorithm to generate a grid of the resistivity data at different depths. The results are presented in Fig. 11a–e. In general, these figures show a decrease in resistivity values with depth. This decrease is attributed to the general fining of the lithologies with depth. The figures show a remarkable variation in resistivity at different depths, probably due to the changes in water content and lithological makeup of the sediments.

The higher resistivity readings with values greater than $100 \Omega\text{m}$ are associated with the gravel-sand facies of the alluvial fans and sandy plain sediments. Where these sediments are dry, the resistivity values can exceed $200 \Omega\text{m}$. These sediments are composed of mixed lithologies ranging in grain size from boulders to fine sands and clays. These deposits are more coarsely grained near the mountains with the grain size gradually decreasing towards the centre of the basin. The sediments comprising the alluvial fans are found in front of the Waziristan-Sulaiman range and the western part of the Bhitanni range, whereas those of sandy plain are found in front of Marwat range. The sands of the sandy plain are medium grained and are the erosional products of the Marwat range. Porosity of the alluvial fan lithologies is low, due to the larger sized particles and poor grading of sediments (Dalfsen et al 1986). With increasing depth the resistivity of these sediments decreases which suggests that the water content increases also and that the lithologies are changing from coarse dry sediments to finer wet sediments.

The sediments from the toes of the alluvial fans towards the basin boundary near Gambila River are deposited in the flood plains. These sediments consist of interbedded fine sand, clay and silt layers. The resistivity of these sediments is found to be in the range of ($15 > \text{Res} < 25 \Omega\text{m}$) and are hence termed as “dirty sand facies.” These sediments fill the majority of the space in the basin and extend to great depths, in general more

Table 2 Variogram parameters

Depth (m)	Model	Nugget	Sill	Range (m)	Nugget (%)	Spatial class
20	Spherical	5,000	26,000	47,532	19.23	Strong
70	Spherical	2,000	8,502	45,551	23.52	Strong
100	Spherical	750	2,800	49,512	26.72	Strong
130	Spherical	500	2,200	71,297	22.72	Strong
150	Spherical	250	1,650	75,258	15.15	Strong

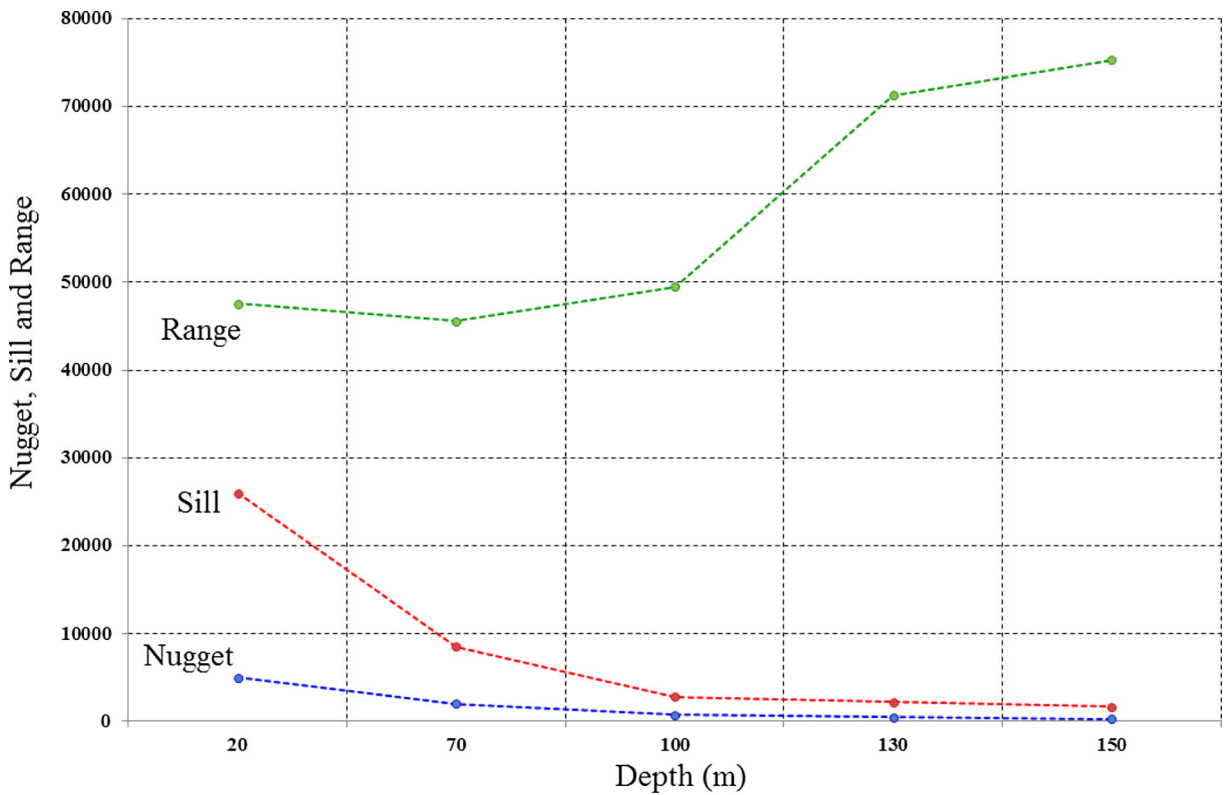


Fig. 10 Spatial correlation of the variogram parameters. *Vertical axis* serves as variability for the nugget and sill where as separation distance for range

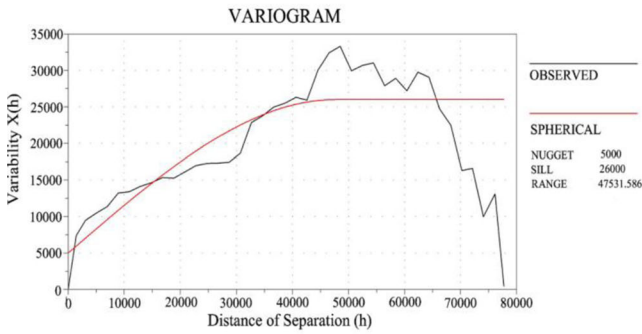
than 100 m as shown in Fig. 11c–e. These sediments are deposited in the flood plains of the Gambila River and its tributaries and are composed of interlayered clay-silt and fine sand. The coarse sediment content in the facies increases towards the Gambila River.

The clay-silt facies ($Res < 15 \Omega m$) covers a considerable portion in the subsurface of the study area and range in variable depth, i.e., 0–150 m as evident from the borehole information. Sometimes this unit lies directly above the dirty sand facies, and somewhere in other locations, it will appear deeper in the basin. It is acknowledged that the saline water content in the subsurface considerably lowers the resistivity of these sediments. Such cases can be observed in Figs. 11 and 12 where the resistivity fall below $5 \Omega m$. Resistivity data interpreted statistically at different depths as shown in Figs. 10 and 11 suggest that the flood plain and lacustrine deposition took place along with Late Quaternary tectonic activity. From Fig. 11b–d, it is observed that the flood plain developed into a lake where clay-silt facies were deposited. The earlier lake was situated towards the south of the area and broadened overtime to occupy more space within the basin. This could have been the

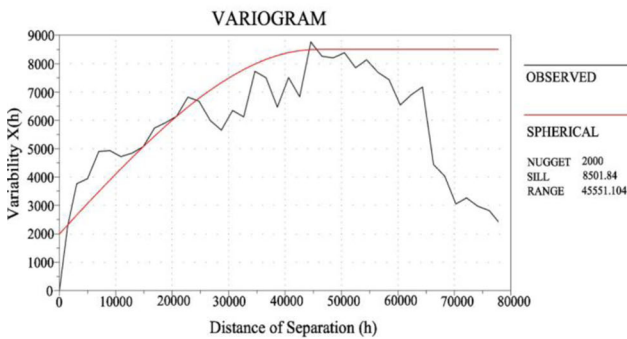
result of rapid uplift of the Bhattani and Marwat ranges, which may have caused the flood plain environment to become lacustrine. The alluvial accumulation in the basin gradually took place by the development of alluvial fans from the Sulaiman and Lakki Marwat ranges along with the flood plains from Gambila River and its tributaries. These sediments are the indicators of the depression where a lake was formed during the Late Quaternary period.

Alluvial stratigraphy

The resistivity cross sections for the profiles AA', BB', and CC' in Fig. 12a–c represent the lithologies as a three layer case. These cross sections are then presented as lithology sections which suggest that the depositional environment has included alluvial fans, flood plains, and lacustrine sediments. The Himalayan orogeny resulted in depressions creating space for sediments derived from the adjacent mountain ranges with the cross sections indicating that the deposition took place in a series of events. The predominance of clay-silt and dirty sand facies throughout the Bannu basin area suggests



a



b

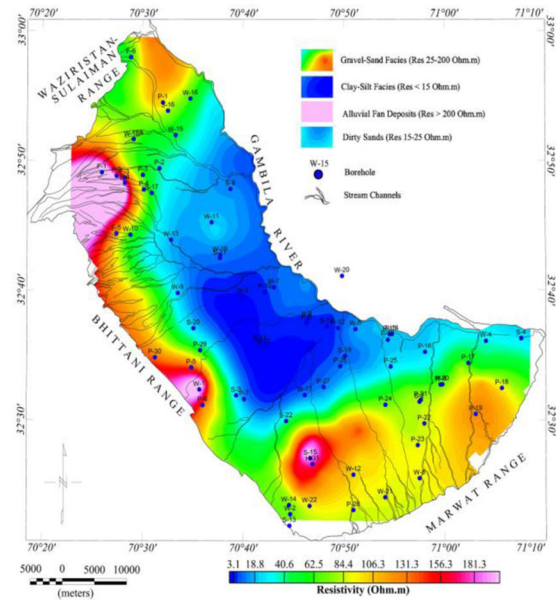
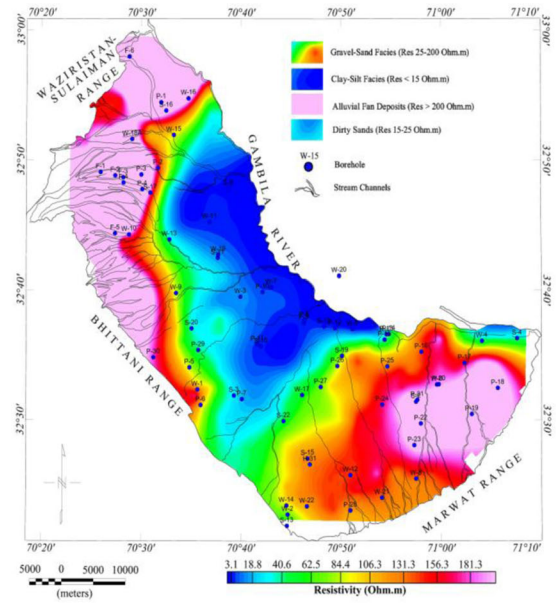
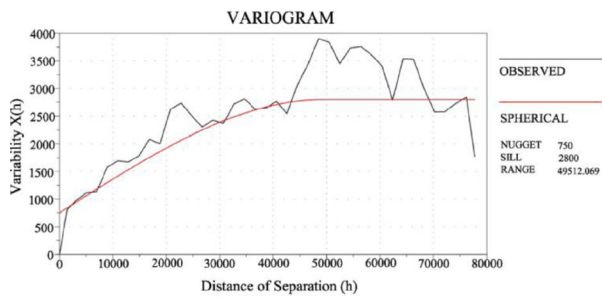


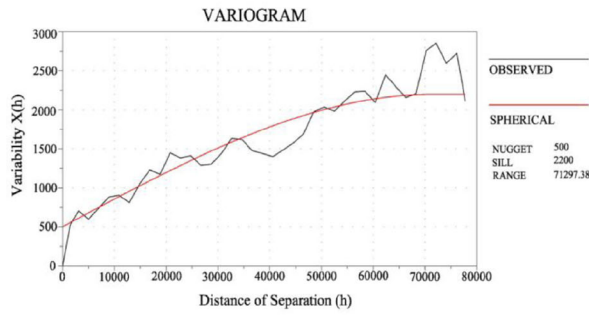
Fig. 11 Variogram and resistivity distribution at **a** 20, **b** 70, **c** 100, **d** 130, and **e** 150am depths

that at the time of deposition a large standing water body such as lake was present. Both of these facies types were significantly eroded and replaced with gravel-sand facies by various stream channels arising in the adjacent mountain ranges. Many boreholes confirm the presence of gravel-sand patches intermixed with sand and silt within these facies as shown in Fig. 12a–c. This is attributed to the stream channels which have reworked the deposited material over time.

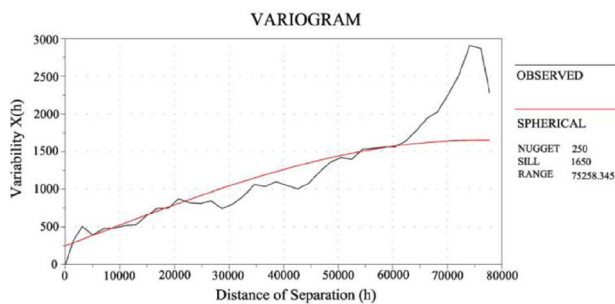
The maps of the resistivity distributions and cross sections of implied lithologies generated by calibrating the borehole lithologies and resistivity soundings correlate together. The maps predict the spatial extent of the geomorphic features where as the cross sections give their variations in a vertical sense. The results of the mapping suggest that the flood plain depositional environment developed into a lake over geologic time as the sedimentation progressed which correlates well with the



c



d



e

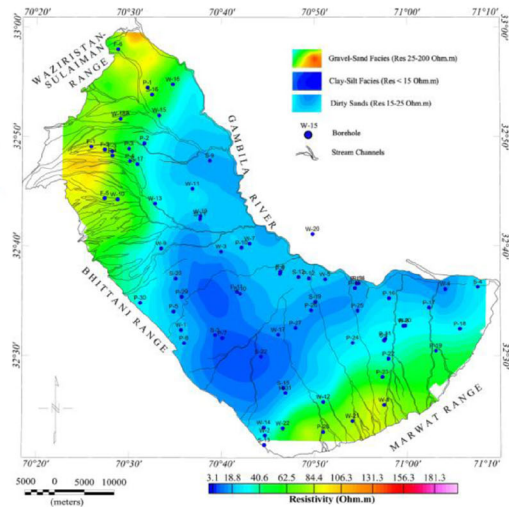
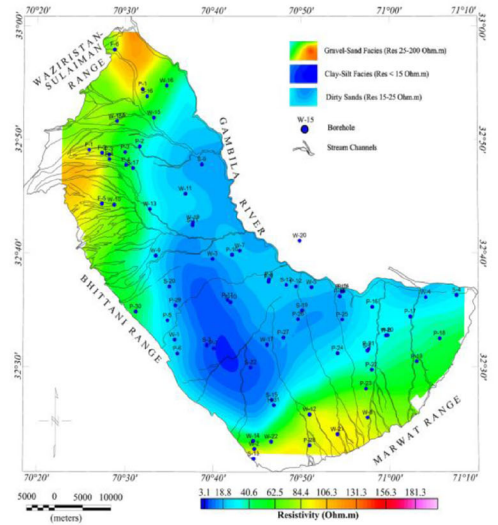
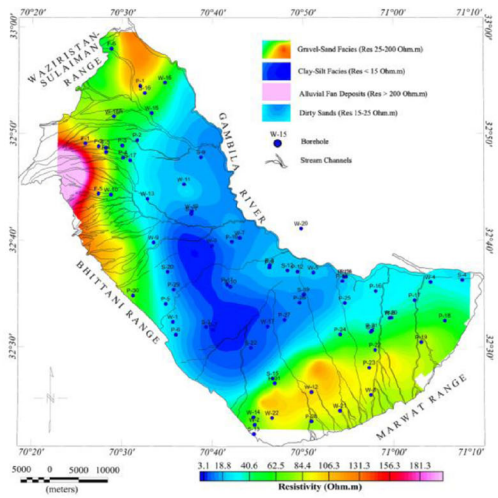


Fig. 11 (continued)

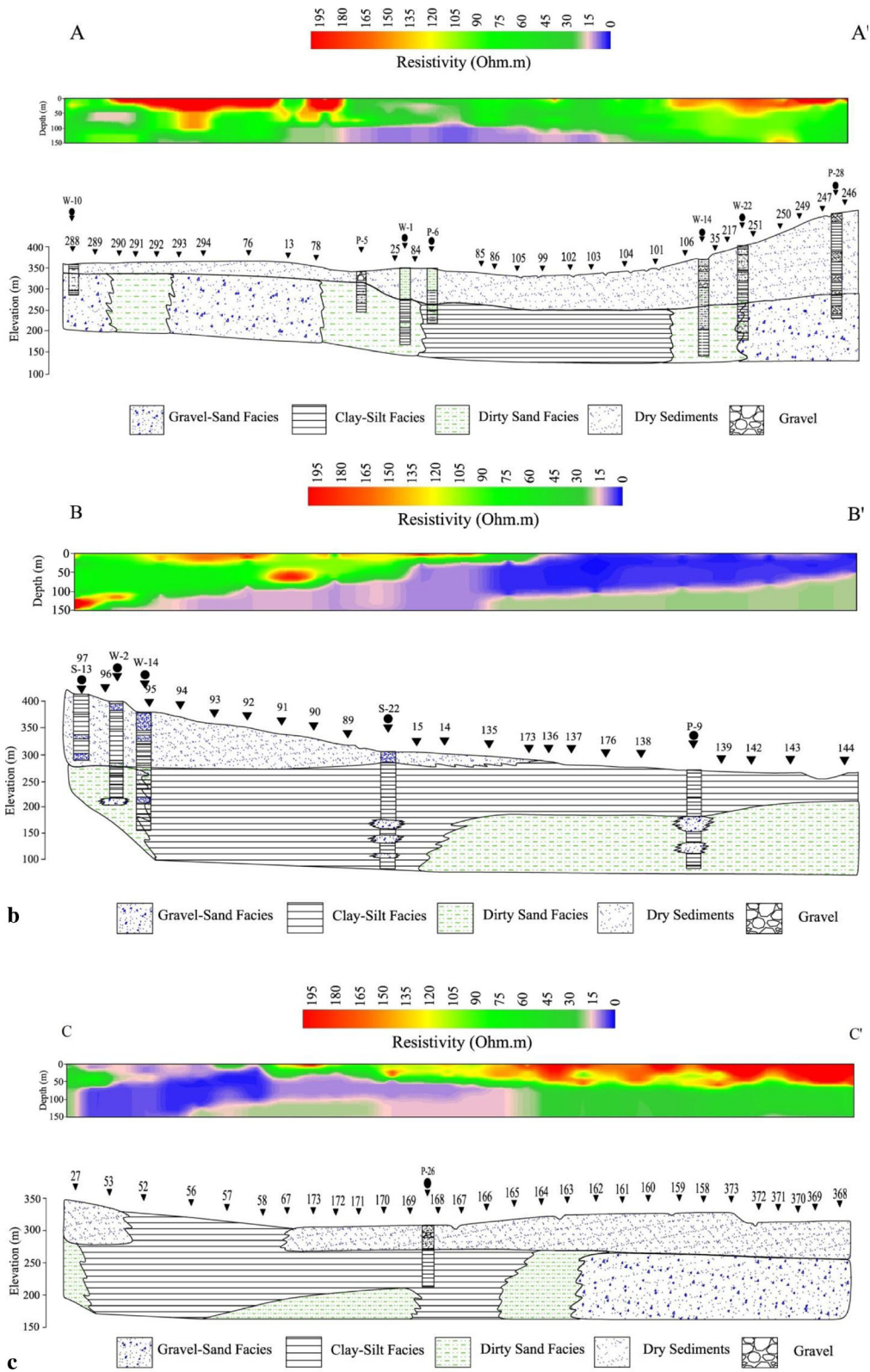


Fig. 12 Stratigraphic cross sections **a AA'**, **b BB'**, and **c CC'** established by calibrated resistivity and borehole data

boreholes data which show massive clay-silt facies above the dirty sand facies. The depression where clay-silt facies were deposited appears to have gradually migrated from south to north and the rate and amount of sedimentation has played a prominent role in shifting of the depression with depth. In general, the depositional sequence starts with the dirty sand facies which is the widespread in the deeper horizons of the whole basin in a flood plain environment. This sequence is followed by the gravel-sand facies arising from the erosion of the adjacent mountains in the form of alluvial fans and sandy plain, whereas the clay-silt sediments evolved in the depressions. The dirty sand facies are significantly eroded and replaced by the gravel-sand facies along the stream channels.

Conclusions

The individual resistivity sounding data that had been collected during the late 1980s in the Bannu basin by WAPDA has been re-worked, modeled, and visualized by using modern geostatistical techniques. The use of variogram aided gridding techniques, more commonly found in seismic modeling and inversion in the petroleum exploration industry, has made it possible to integrate the data into a single basin wide study. The VES data was originally processed as individual resistivity soundings with limited scope for any geological interpretation; however, the remodeled data can now be interpreted to reveal gross subsurface lithologies, geomorphologies, and depositional patterns.

For the area being studied, tuning of the variogram and gridding parameters has made it possible to identify individual lithologies such as alluvial fans and stream channels based on inferred grain sizes, depositional style, and geomorphological features. Sequences of coarse grained sediments were recognized near the mountain ranges, with the sediments fining towards the center of the basin. Two lithology types were differentiated within the central plain and their lateral and vertical extents were identified and mapped. The shallow region in the centre of the study area is characterized by alternating bands of silt layers with clay layers of variable thickness. The presence of these lithologies indicates the location of the body of standing water in which they originated such as a lake, and document their positional changes over time as the sedimentation progressed. The deeper region is characterized by

alternating bands of silt, clay, and sand layers belonging to the flood plain deposits. The presence of gravels in boreholes and their associated facies observed in the mapping suggest that braided channels were present which can serve as good sources of water supply, if developed. The subsurface along the mountain ranges comprise gravel-sand facies consisting of layers of gravels, pebbles and sand intercalated with clay beds. These layers comprise the alluvial fans intruding into the basins. Coarse and fine sediment beds alternate, with the coarse layers being most dominant.

References

- Akhter, G., Farid, A., & Ahmed, Z. (2012). Determining the depositional pattern by resistivity-seismic inversion for the aquifer system of Maira Area, Pakistan. *Environmental Monitoring and Assessment*, 184, 161–170.
- Armstrong, M. (1984). *Improving the estimation and modeling of the variogram* (pp. 1–20). Dordrecht: Geostatistics for Natural Resources Characterization; Reidel.
- Bowling, C. J., Rodriguez, B. A., Harry, D. L., & Zheng, C. (2005). Delineating alluvial aquifer heterogeneity using resistivity and GPR data. *Ground Water*, 43(6), 890–903.
- Bowling, C. J., Harry, D. L., Rodriguez, B. A., & Zheng, C. (2007). Integrated geophysical and geological investigation of heterogeneous fluvial aquifer in Columbus Mississippi. *Journal of Applied Geophysics*, 62(1), 58–73.
- Cambardella, C. A., Moorman, T. B., Vovak, J. M., Parkin, T. B., Karlen, D. L., Turco, R. F., et al. (1994). Field scale variability of soil properties in Central Iowa Soils. *Soil Science Society of America Journal*, 58(2), 1501–1511.
- Courteaud, M., Ritz, M., Robineu, B., Join, J. L., & Coudray, J. (1997). New geological and hydrogeological implications of the resistivity distribution inferred from audiomagnetotellurics over La Fournaise young shield volcano (Reunion Island). *Journal of Hydrology*, 203(1–4), 93–100.
- Cressie, N. (1993). *Statistics for spatial data*. New York: Wiley. 900.
- Dalhsen, W. V., Riaz, M., & Nadeem Ul Haq. (1986). Technical report of groundwater resources in Lakki Marwat Area, Bannu District, N. W. F. P, Report No. IV-3.
- Edmund, A. (2009). Hydrogeological deductions from geoelectric survey in Uvwiamuge and Ekakpamre communities, Delta State, Nigeria. *International Journal of Physical Sciences*, 4(9), 477–485.
- Farid, A., Jadoon, K., Akhter, G., & Iqbal, M. A. (2013). Hydrostratigraphy and hydrogeology of the western part of Maira area, Khyber Pakhtunkhwa: a case study by using electrical resistivity. *Environmental Monitoring and Assessment*, 185(3), 2407–2422.
- Geosoft Oasis Montaj. (2013). Software for earth science mapping and processing, Geosoft Incorporation Ltd.
- Goovaerts, P. (1997). *Geostatistics for natural resources evaluation*. New York: Oxford University Press. 483.

- Gringarten, E., & Deutsch, C. V. (2001). Teacher's aide: variogram interpretation and modelling. *Mathematical Geology*, 33(4), 507–534.
- IPI2WIN-1D computer programme. (2000). *Programs set for 1-D VES data interpretation*. Moscow: Department of Geophysics, Geological Faculty, Moscow University.
- Iqbal, J., Thomasson, J. A., Jenkins, J. N., Owens, P. R., & Whisler, F. D. (2005). Spatial variability analysis of soil physical properties of alluvial soils. *Soil Science Society of America Journal*, 69(4), 1338–1350.
- Journel, A. G., & Huijbregts, C. J. (1978). *Mining geostatistics*. New York: Academic Press. 600.
- Kazmi, A. H., & Jan, M. Q. (1997). *Geology and tectonics of Pakistan*. Graphic Publishers, 5C-6/10, Nazimabad, Karachi.
- Louis, I. F., Louis, F. I., & Grambas, A. (2002). Exploring for favorable groundwater conditions in hard rock environments by resistivity imaging methods: synthetic simulation approach and case study example. *Journal of Electrical and Electronics Engineering*, Special issue, 1–14.
- Okoro, E. I., Egboka, B. C. E., & Onwuemesi, A. G. (2010). Evaluation of aquifer characteristics of Nanka sands using hydrogeological method in combination with vertical electrical sounding (VES). *Journal of Applied Science and Environmental Management*, 14(2), 5–9.
- Olea, R. A. (1995). Fundamentals of semivariogram estimation, modeling and usage, Stochastic modeling and geostatistics: principles, methods and case studies, AAPG computer. *Applications in Geology*, 3, 27–36.
- Riddell, E. S., Lorentz, S. A., & Kotze, D. C. (2010). A geophysical analysis of hydro-geomorphic controls within a headwater wetland in a granitic landscape, through ERI and IP. *Hydrology and Earth Systems Sciences*, 14, 1697–1713.
- Schrott, L., & Sass, O. (2008). Application of field geophysics in geomorphology: advances and limitations exemplified by case studies. *Geomorphology*, 93(1–2), 55–73.
- Searle, M. P., Khan, M. A., Jan, M. Q., DiPietro, J. A., Pogue, K. R., Pivnik, D. A., et al. (1996). Geological Map of North Pakistan and adjacent areas of northern Ladakh and Western Tibet (Western Himalaya, Salt ranges, Kohistan, Karakoram and Hindi Kush).
- Shahzad, F., Mahmood, S. A., & Gloaguen, R. (2009). Drainage network and lineament analysis: an approach for Potwar Plateau (northern Pakistan). *Journal of Mountain Sciences*, 6(1), 14–24.
- Shahzad, F., Mahmood, S. A., & Gloaguen, R. (2010). Nonlinear analysis of drainage systems to examine surface deformation: an example from Potwar Plateau (Northern Pakistan). *Nonlinear Processes in Geophysics*, 17(2), 137–147.
- Stewart, M., Layton, M., & Theodore, L. (1983). Application of resistivity surveys to regional hydrogeologic reconnaissance. *Ground Water*, 21(1), 42–48.
- Sultan, S. A., Mekhemer, H. M., Santos, F. A. M., & Abd Alla, M. (2009). Geophysical Measurements for subsurface mapping and groundwater exploration at the central part of the Sinai Peninsula, Egypt. *The Arabian Journal for Science and Engineering*, 34(1A), 103–119.
- Vogelsang, D. (1995). *Environmental geophysics: A practical guide*. Berlin: Springer.
- Zananiri, I., Memou, T., & Lachanas, G. (2006). Vertical electrical sounding (VES) survey at the central part of Kos Island, Aegean, Greece. *Geosciences*, 411–413.
- Zouhri, L., Gorini, C., Mania, J., Deffontaines, B., & Zeroulai, A. (2004). Spatial distribution of resistivity in the hydrogeological systems, and identification of the catchment area in the Rharb basin, Morocco. *Hydrological Sciences-Journal-des Sciences Hydrologiques*, 49(3), 387–398.